DYNAMIC ANALYSIS OF VOLTAGE MODE BUCK CONVERTER

FINAL PROJECT FOR ELEC 835

XIANG ZHANG

Table of Contents

1. Introduction, classification, and methodology 2
1.1 Techniques for Complex behavior research in DC-DC switching converters 2
1.2 Complete system state equation method 4
1.3 Discrete iterative nonlinear mapping 5
1.4 Tools for virtualization and description of chaos dynamic characteristics in DC-DC switching converters 7
a). Lyapunov exponent 7
b). Jacobian matrix near the equilibrium point 8
c). Poincaré map, bifurcation diagram, strange attractor 9
2. Complex behavior and its analysis in CCM VCM buck converter 11
2.1 Complete system state equation for CCM VCM buck converter 12
2.2 The structurable numerical modeling in Matlab 12
Non-autonomous system 14
2.3 Analysis using bifurcation diagram and Poincaré map 15
a). Vin as bifurcation parameter 16
b). L as bifurcation parameter 17
c). C as bifurcation parameter 17
Analysis using Poincaré map 17
2.4 Theoretical analysis using iterative mapping 18
Jacobian matrix stability criteria 20
2.5 Complex behavior verification using PSIM 21
3. Complex behavior and its analysis in DCM VCM buck converter 24
3.1 Discrete iteration mapping for DCM Buck 24
Approximation in discrete iteration mapping 25
3.2 Stability analysis cobweb map and bifurcation diagram 26
a). System behavior predicts using cobweb map 27
b). System behavior predicts using bifurcation diagram 28
3.3 Determine threshold for the first fork bifurcation 29
3.4 Complex behavior verification using PSIM 29
4. Possible applications of complex behavior buck converter 31
5. Conclusion 32
6. References 32

1. Introduction, classification, and methodology

DC-DC switching converter is an important part of power electronics. In its traditional research process, researchers rarely involve nonlinear phenomena in their studies, but in the actual design process of switching converter, sometimes it is nonnegligible for a special operational condition, some perform abnormal phenomena that the traditional linear system description method cannot explain, which indicates the existence of chaos phenomenon.

However, many engineering designers often simply take this phenomenon as unknown interference in the converter, even though some experienced designers can change the circuit parameters to avoid or diminish this phenomenon, theorizing these engineering techniques are still a challenge.

To lead the practical experiment and eliminate the aforementioned complex behavior concerning DC-DC converters. some rapid development of chaotic phenomenon research has been processed all over the world, and many achievements have been obtained. This report will give a fundamental glimpse to these results, especially relating to the most widely deployed voltage-mode controlled buck converters, including its complex behavior bifurcations referring to parameter varying, chaos phenomenon research methods in DC switching converters, etc.

1.1 Techniques for Complex behavior research in DC-DC switching converters

To reveal the nonlinear dynamic behavior of the converter, the key issue is to establish a corresponding dynamic model with an appropriate method. At present, two analysis methods are mainly used: the first one is to derive the state equation directly according to the topology morphing of the system, using KCL law and KVL law to establish a unified state equation model, and then perform accurate model simulation; t the other one is to derive the system state discrete iterative nonlinear mapping of the

system state variable, by deriving its Jacobian matrix, computing eigenvalues to determine the system characteristics and stabilities.

Among them, the former can obtain all the dynamic behavior of the conversion system, which tends to be only a numerical calculation for the accurate model, but it needs an extremely large amount of calculation for both significant and trivial complex behaviors are required to be observed; while the latter can be used to analyze the stability of the system, but it is generally only suitable for the analyzing of the first bifurcation fork. In short, these two analytical research tools are technically complementary, when dealing with a practical system.

Table 1.1. Comparation for two different analysis techniques

	Complete system state equation	Discrete iterative nonlinear mapping
Pros	Accurate, all complex dynamic behavior are visible	Small calculation complexity, stability criteria can be easily found
Cons	Large calculation complexity, numeric simulation relies on sufficient resolution	Only suitable for first fork analysis in general
Visualization	Phase Portrait Bifurcation Plot (sampling) Poincaré Map (sampling)	Bifurcation Plot Poincaré Map Iterative map

The above chart shows the technique comparison of the complete system state equation method and the discrete iterative nonlinear mapping, we can see that both methods have their advantages and limitations, but the visualization tools can overlap. This is important for our further study, since the bifurcation and chaos phenomenon should be visualized, otherwise it will be difficult separating the traditional dynamic system to the chaos system.

1.2 Complete system state equation method

The DC-DC converter is a typical piecewise linear system. According to the different switching states, Buck converters, Boost converters, Buck-Boost converters, etc. generally have two or three operating modes, the former is called continuous conduction mode (CCM, composed of two piecewise linear systems), the latter is called discontinuous conduction mode (DCM, consists of three piecewise linear systems). Continuous conduction mode requires that the inductance in the circuit be large enough, if the inductance is less than a certain parameter value, it will switch to discontinuous conduction mode.

The operating mode of the circuit can usually be determined by observing the waveform of the inductor current. If we set d to be the duty cycle and T_s to be the switching period. Figure 1.1 shows the continuous and discontinuous state of the inductor current. It can be known from analyzing the current waveform diagram that in a switching cycle T_s, the dT_s segment indicates that the switch S is turned on, and the diode D is turned off; $d'T_s$ section indicates that switch S is turned off and diode D is turned on; section $d''T_s$ indicates that both switch S and diode D are turned off; and in discontinuous mode, $dT_s + d'T_s + d''T_s = T_s$ is established.

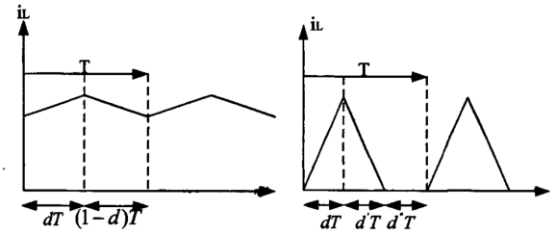

Figure 1.1. The model of circuit

(a) continuous model (b) discontinuous model

According to the switching state, we can obtain the state equation of the switching converter, which is written as

$$\dot{x} = A_j x + B_j V_{in} \quad 1.1$$

where x is set as a state variable, A_j B_j, is the coefficient matrix corresponding to a piecewise linear system, and has:

(1) When j=1 ($0 < t < dT_s$), the switch is on and the diode is disconnected;

(2) When j=2 ($dT_s < t < d'T_s$), the switch is off and the diode is closed;

(3) When j=2 ($d'T_s < t < d''T_s$), the switch and diode are both disconnected.

The advantage of this method is that it does not require simplification and approximation of the circuit system, the established equation is an accurate model of the circuit system, and the solution of the equation reflects the real physical characteristics of the system; but the disadvantage is that it is difficult to analyze the dynamics of the system by analytical methods. Learning behaviors such as the stability of various bifurcations and periodic orbits can generally only be solved numerically.

1.3 Discrete iterative nonlinear mapping

At present, most literatures use nonlinear discrete-time mapping based on the concept of discrete-time model when analyzing the nonlinear phenomenon of converters, that is, the state of the converter is mapped from one sampling time to the next sampling time. This method is used in applications with many advantages in computer numerical calculation and reduction of computational load and can successfully analyze the stable working state of the converter, bifurcation and other phenomena.

According to the selection of different sampling times of the converter, discrete time mapping can generally be divided into four types, namely stroboscopic mapping, synchronous switching mapping, asynchronous switching mapping, and pair-switching mapping [1].

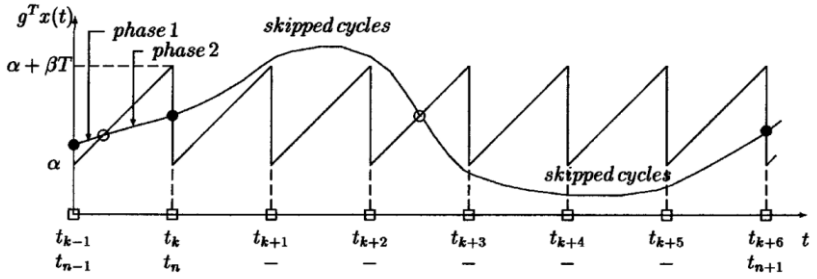

Figure 1.2. Illustration of stroboscopic mapping and synchronous switching mapping

The first three mappings can be seen in Figure 1.2 (assuming that the converter is in continuous conduction mode, there are two phase states corresponding to different switching topologies) where the stroboscopic mapping is performed on the converter state at the beginning of each PWM cycle. sampling, thus constructing a mapping to iterate the state of the converter from one cycle to the next. This mapping method is widely used in the study of nonlinear phenomena of converters because of its intuitive and convenient construction.

At an integral multiple of the switching period T_S, the converter may not have phase switching, but a skipped period occurs, and the stroboscopic mapping cannot be correctly distinguished, so the concept of synchronous switching mapping is proposed, which is only in the switching period T_S. The state variable is sampled only when the phase of the converter is switched at an integer multiple times (synchronized switching), so it is possible to distinguish between the phase switching period and the jumping period [2].

Asynchronous switching mapping [3] can analyze the situation of multi-pulse M. This mapping samples the converter state at the phase switching time (i.e., the asynchronous switching time) within the switching cycle, so its sampling time is not synchronized with the switching cycle, and the paper [3] constructed the mapping from one asynchronous switching moment to the next asynchronous switching moment by taking the converter state variable and duty cycle as the mapping variables. Based on this, the analytical conditions for bifurcation in the converter were obtained.

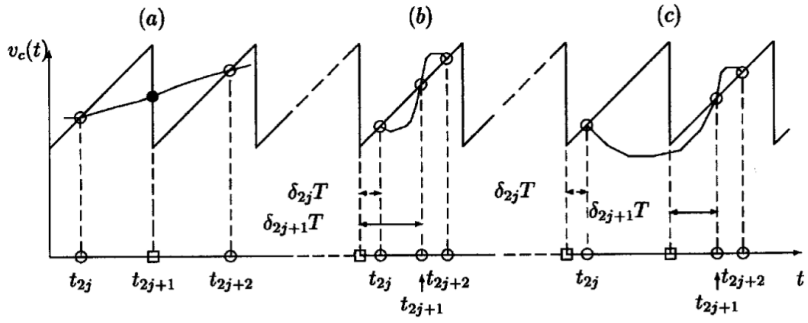

Figure 1.3. The circumstances of two-by-two mapping

When there is no trigger in the feedback loop, multiple phase switching may occur in one switching cycle (i.e., multi-pulse phenomenon, as shown in Figure 1.3). Currently,

the most reasonable analysis method is to use paired switching mapping. The phase switching process of the converter is always fixed, that is, after an initial time t_{2j}, the converter is in phase 1, and the phase remains unchanged until t_{2j+1}, then the converter switches to phase 2 in the interval (t_{2j+1}~t_{2j+2}), and then start the next round of phase switching, so that the switching sequence "phase 1-phase 2" constitutes a paired phase, the paired switching mapping is the state of the sampling phase pair at the initial moment, thus forming a phase pair interval mapping for the state variable.

The advantage of this method is that it is easy to comprehensively analyze the dynamic properties of the circuit system, such as the stability of fixed points and various periodic orbits, the boundary collision bifurcation and the period-doubling bifurcation belonging to the high-frequency domain; but the disadvantage is that the circuit system must be simplified and approximated in order to derive its discrete iterative nonlinear mapping. This makes the dynamic properties of the discrete model different from that of the actual circuit system. Besides, only the one-dimensional mapping can obtain a closed-form, and the two-dimensional mapping can only be obtained by numerical methods in general (for a kind of special structure The closed-form two-dimensional mapping of the switching power converter can be obtained).

1.4 Tools for virtualization and description of chaos dynamic characteristics in DC-DC switching converters

In the study of chaos in DC-DC switching converters, power spectrum analysis, Lyapunov exponent, Jacobian matrix, bifurcation diagram, Poincaré map, and Geometric analysis of strange attractors is the commonly used analysis and description methods.

a). Lyapunov exponent

For a dynamic system, the adjacent orbits can be stretched or compressed during the evolution of the system, and their rates may be different at different points in the phase space. Only by taking a long-term average of the stretching or compression rates at each

point the motion of trajectory dynamics can be described. This overall effect of the system is the concept of the Lyapunov exponent.

The positive Lyapunov exponent indicates that the orbit is unstable in each part, the adjacent orbits are exponentially separated, and the orbit is repeatedly folded under the action of the overall stability factor (bounded, dissipation), forming Chaos attractor. An n-dimensional map has n stretching or compression directions, each of which corresponds to a Lyapunov exponent.

Generally, in the study of nonlinear characteristics of second-order converters, the concept of the maximum Lyapunov exponent is mostly used. The maximum Lyapunov exponent can correspond to three different situations: less than 0, the converter dynamics are periodic; equal to 0, the converter The dynamic is quasi-periodic; and greater than 0 indicates that the converter is in chaotic dynamic [4].

b). Jacobian matrix near the equilibrium point

The Jacobian matrix can be used to analyze the nonlinear characteristics of the converter system [5]. There are two methods: one is to establish the Jacobian matrix of the periodic mapping, and the other is to establish the Jacobian matrix of aperiodic fixed points.

The common method is the former: a certain parameter A of the converter is selected as the bifurcation parameter, and the explicit discrete iterative mapping of the DC/DC converter can be written as

$$x_{n+1} = f(x_n, A) = \begin{bmatrix} f_1(v_n, i_n, A) \\ f_2(v_n, i_n, A) \end{bmatrix} \tag{1.2}$$

Where $x_n = [v_n, i_n]^T$ is the state variables of iterative map.

Then the Jacobian matrix will be:

$$J_f(x_Q) = \begin{bmatrix} \frac{\partial f_1}{\partial v_n} & \frac{\partial f_1}{\partial i_n} \\ \frac{\partial f_2}{\partial v_n} & \frac{\partial f_2}{\partial i_n} \end{bmatrix} \tag{1.3}$$

In the formula, x_Q is the equilibrium point of the discrete time periodic mapping, and the characteristic equation of the converter is

$$det[\lambda I - J_f]|_{x_n = x_Q, A_n = A_Q} = 0 \tag{1.4}$$

Solving this equation, the value of A whose characteristic value is -1 is the bifurcation point (that is, the bifurcation from the period 1 orbit to the period 2 orbit); Similarly, if the second bifurcation occurs in the converter (that is, the bifurcation from the period 2 orbital to the period 4 orbital), the eigenvalue of the discrete-time map $f[f(x_n, A)]$ is set at the -1.

c). Poincaré map, bifurcation diagram, strange attractor

Poincaré invented a method to describe the structure of strange attractors. This method is to cut a two-dimensional cross section from the strange attractors, which is called Poincaré cross-section.

On this section, the orbit first produces an intercept point x_1, and the next period it intersects the section on x_2, so it is called as x_1 is mapped to x_2, likewise, x_2 will be mapped to x_3 . . . This establishes the mapping relationship between discrete point x_n:

$$x_{n+1} = f(x_n) \quad 1.5$$

This mapping is called the Poincaré map. The Poincaré section makes the complex motions observable through the Poincaré map, which greatly simplifies the problem. This section reduces the dimension of the attractor by one dimension, transforms the continuous time evolution into a discrete map, which compresses a lot of secondary information and is easy to handle mathematically, which brings great convenience to research.

If the system performs simple periodic motion, then the orbit passes through the section at the same place each time, and there is only one fixed point on the section; if it is 2 times the period, there are two intercept points on the section, and if it is 4 times the period, there are 4 intercept points on the section. point. If the system performs quasi-periodic motion, then the intersection points on the section constitute a closed curve; if the motion is aperiodic, there will be infinitely many points on the section. Therefore, from the Poincaré section, the nature of the motion of the system can be immediately judged quality. Figure 1.4(a) shows the Poincaré cross-section.

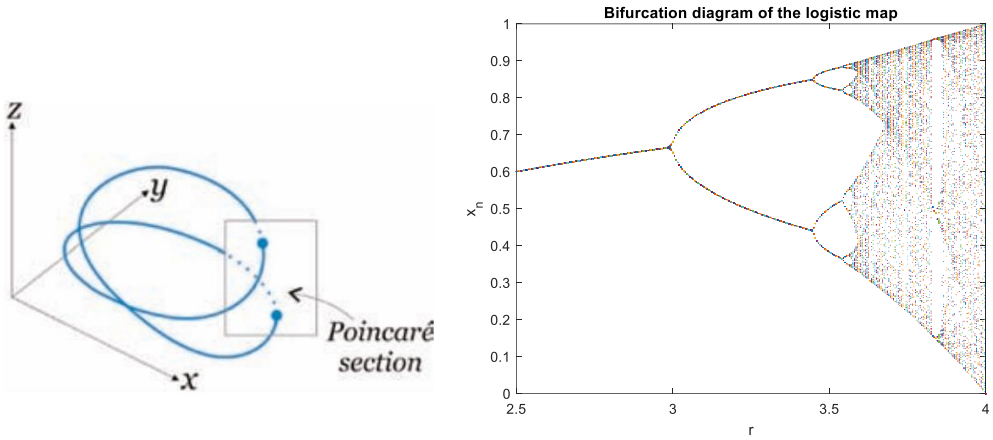

Figure 1.4 (a) Poincaré section (b) bifurcation diagram

Similarly, the bifurcation graph also plays an important role in the nonlinear dynamic research of the converter. The construction method is based on the Poincaré section generated by discrete-time mapping. A certain state variable of the Poincaré section can be selected as the bifurcation diagram. One-dimensional coordinates in the bifurcation diagram and the other dimension of the bifurcation graph correspond to the change of bifurcation parameters.

In this way, the bifurcation diagram can provide an overview of the changes in the dynamic characteristics of the system as the parameters change. DC-DC. The dynamic characteristics of the DC switching converter may change with the change of any adjustable parameter value. Therefore, there are many kinds of bifurcation parameters in the bifurcation diagram. The PWM period, circuit element parameter values, and reference signal can be considered. value, feedback loop factor, etc. Figure 1.4(b) shows the bifurcation diagram of the logistic map.

2. Complex behavior and its analysis in CCM VCM buck converter

The voltage-mode control Buck converter is a DC-DC converter with voltage as the control object. Its basic circuit topology is redrawn in Figure 2.1(a). It is a typical PWM control system, which may produce various linear and nonlinear phenomena, such as bifurcation, chaos, boundary collision, cataclysm, intermittent, attractor coexistence, etc.

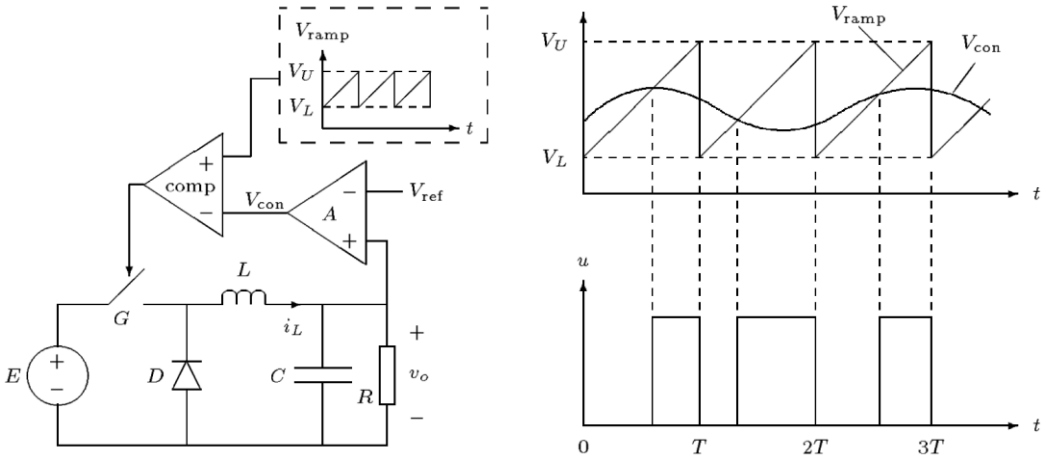

Figure 2.1. Voltage mode buck converter

(a) Circuit diagram **(b) The key waveform**

Its main circuit consists of an inductor, capacitor, switch, diode, and load resistor respectively. In order to facilitate the analysis of the working principle of the circuit, it is necessary to make two approximations:

(1) Assuming switch G and diode D are ideal switching devices, that is, they can be "on" and "off" instantaneously, when "on" occurs, and the voltage is 0V when "off" occurs, and the current is 0A;

(2) Assuming the capacitor and the inductor are ideal components without parasitic parameters.

2.1 Complete system state equation for CCM VCM buck converter

According to the different states of switch G, the topology of the buck converter changes, there are two main circuit topologies corresponding to the two states of switch G:

When u=1, the switch G is closed, the diode D is subjected to the reverse voltage and turned off, and the input power Vin and the inductor L and the RC output part are connected in series, this is the energy input stage, and the current rises almost linearly; When u=0, the switch G is turned off, the diode D is turned on under the forward voltage, and the inductor L is only connected in series with the RC output part, forming a path for the inductor current, and the inductor current decreases almost linearly through the diode and the load.

The differential equations corresponding to the above two main circuit topologies can be described as:

$$\dot{x} = \begin{bmatrix} -/RC & 1/C \\ -1/L & 0 \end{bmatrix} x + \begin{bmatrix} 0 \\ 1/L \end{bmatrix} V_{in} = A_{on}x + B_{on}V_{in} \quad \text{when G is on} \tag{2.1}$$

when G is on

$$\dot{x} = \begin{bmatrix} -/RC & 1/C \\ -1/L & 0 \end{bmatrix} x + \begin{bmatrix} 0 \\ 0 \end{bmatrix} V_{in} = A_{off}x + B_{off}V_{in} \quad \text{when G is off} \tag{2.2}$$

$x = [Vo\ i_L]^T$ is the state-variables for the system, and A and B are the coefficient matrix of the system.

According to these two equations in the formula, the unified state equation including the control signal S can be described as:

$$\dot{x} = \begin{bmatrix} -/RC & 1/C \\ -1/L & 0 \end{bmatrix} x + \begin{bmatrix} 0 \\ V_{in}/L \end{bmatrix} S(d) \tag{2.3}$$

2.2 The structurable numerical modeling in Matlab

Generally, the closed-loop control system of the DC-DC switching converter belongs to the PWM system, which is a non-autonomous nonlinear system. When we establish its numerical simulation model, there are two methods that can be used: one is to ignore the time variables and establish the autonomous system model which can be used for

numerical simulation and dynamic characteristic analysis; another method is that time can also be regarded as a state variable to establish the non-autonomous system model of the converter.

On the basis of the circuit analysis of the aforementioned buck converter and considering the definition of autonomous and non-autonomous systems, we can establish its numerical simulation model. The following simulation uses Matlab Simulink as a tool to introduce numerical simulation.

According to the different control signals $S(d)$ of the switch G, the converter has two working states, as shown in formula below. Unifying these two cases, the variable structure differential equation of the converter can be obtained as:

$$\dot{Vo} = \frac{i_L - Vo/R}{C} \tag{2.4}$$

$$\dot{i_L} = \frac{S(d)Vin - Vo}{L} \tag{2.5}$$

We also need the equation to relate feedback with control signal $S(d)$. in the voltage mode control mode, this relationship is constructed by amplifying the error signal: difference between output voltage Vo and V_{ref}, to generate control voltage signal V_{con}, we can write this as:

$$V_{con}(t) = K\left(Vo - V_{ref}\right) \tag{2.7}$$

Where the K is the amplifying gain, then by comparing this V_{con} with a clock ramp $Vramp$, the comparing output will be the control signal $S(d)$.

$$Vramp(t) = V_L + (V_U - V_L)t/T_s \tag{2.8}$$

$$S(d) = \begin{cases} u = 0 & when\ Vramp < V_{con} \\ u = 1 & when\ Vramp > V_{con} \end{cases} \tag{2.9}$$

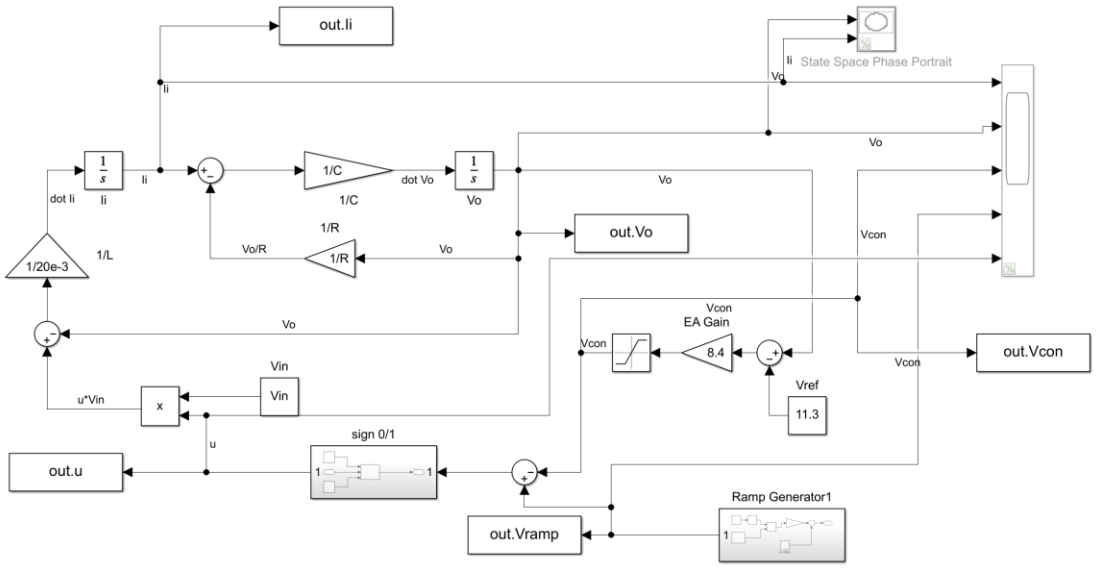

Figure 2.2. Simlink model of CCM buck under voltage mode control

According to equation (2.4, 2.5), the accurate Simulink segment switch model of Buck converter was constructed, as shown in Figure 2.2, in which two integral modules Vo and i_L are used to realize the two differentials of equation (2.4, 2.5). Submodule ramp generator produce the sawtooth wave signal with a period of T_s, the control voltage signal V_{con} realizes the formula (2.7), and the control signal $S(d)$ in the formula (2.9) is finally obtained by using the subtraction between the two signals.

Non-autonomous system

In essence, the PWM control system is a non-autonomous dynamic system, the description equation contains time variables. For example, the sawtooth wave in the Buck converter is a periodic signal related to time, see equation (2.10). In the non-autonomous system model of the buck converter, the structure of the sawtooth sub-module $Vramp$ is shown in Figure 2.3. The output of the integration module is the result of integrating the constant l, that is, the time variable t is obtained. In the following simulation or calculation, we will replace the time variable t with the output $Vramp$.

$$Vramp(t) = V_L + (V_U - V_L)t/T_s(mod1) \qquad 2.10$$

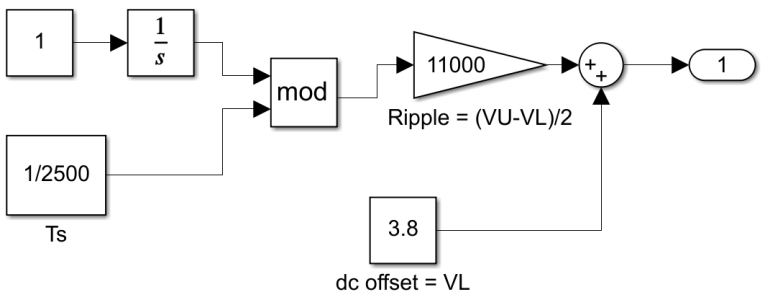

Figure 2.3. autonomy model of sub-module V_{ramp}

2.3 Analysis using bifurcation diagram and Poincaré map

The elements value we choose to running the simulation are as follows: $V_{in} = 20\sim35V$, L=10~20mH, C=20~80μF, R=22 Ω, K=8.3, Ts=400 μs, V_L=3.8 V, V_U = 8.2 V, it should noted that while runing the simulations to generate the bifurcatio map, only one parameter in all the parameters can varing.

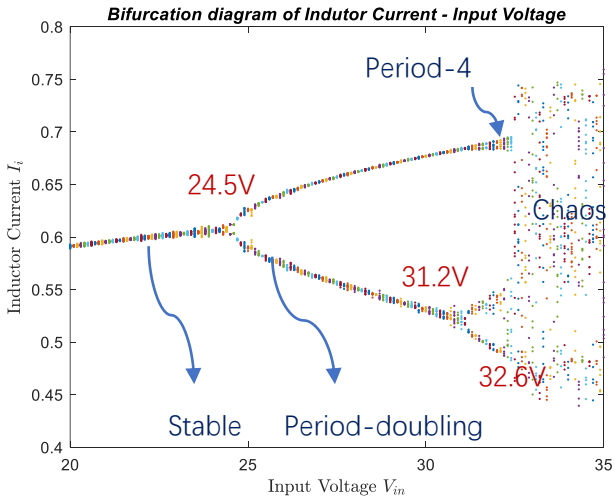

(a) V_{in} as bifurcation parameter

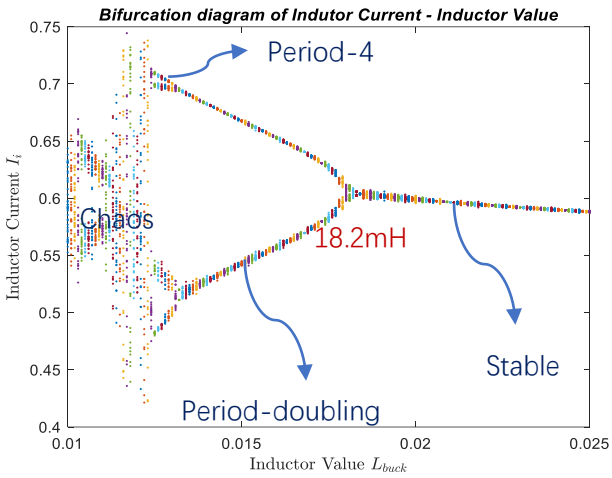

(b) L as bifurcation parameter

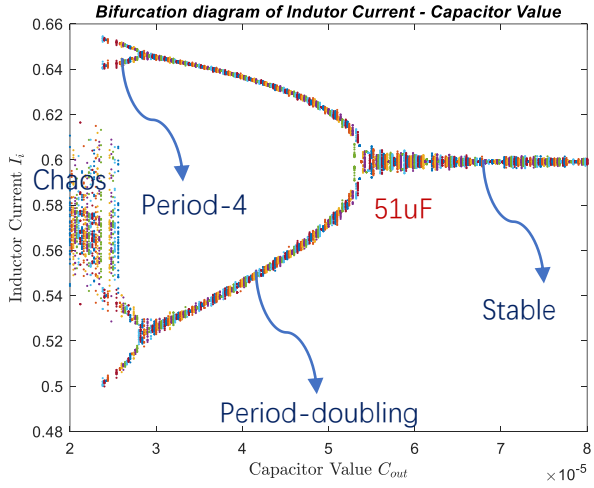

(c) C as bifurcation parameter

Figure 2.4. Bifurcation diagram with (a) V_{in} (b) L (c) C as bifurcation parameter

a). V_{in} as bifurcation parameter

In the bifurcation diagram with the input voltage V_{in} as a parameter, we can find a variety of complex bifurcation behavior. First, it can be seen from the main bifurcation line that there is a period-doubling bifurcation; secondly, the main bifurcation finally undergoes a radical change at $V_{in} \approx 32.6V$ and enters into chaos; in addition, at the same time as the main bifurcation begins, three attractors can be found. The coexistence phenomenon is most obvious and has a clear bifurcation structure when the input voltage

V_{in} is between 31.2V and 32.6V, which is the bifurcation structure starting with period 6, and the two coexisting bifurcations both eventually develop towards a chaotic state.

b). L as bifurcation parameter

In the bifurcation diagram with the inductance L as the parameter, we can find that when the value of the inductance is small, the system is in chaos operation.

With the increase of the inductance L, the system enters period-four bifurcation from chaos, then it evolute to the period-doubling bifurcation, until L≈18.2mH, the system goes stable. At the same time when the main fork exist, it can also be found that there are several attractors coexist.

c). C as bifurcation parameter

In the bifurcation diagram with capacitance C as the parameter, we can find that when the value of capacitance is small, the system is in chaos operation.

With the increase of capacitance C, the system enters period-four and then period-doubling bifurcation from chaos. When C≈28μF, the system is in cycle two, the system is stable when C≈30μF; at the same time as the main bifurcation, it can also be found that there are coexistence of attractors in many places, too.

Analysis using Poincaré map

The essence behind the Poincaré map is much like the bifurcation diagram, which is thoroughly explained in the introduction part. By mapping the states variables to a section plane, the strange attractors can be easier to virtualized.

In this part we only plot the most obvious example Poincaré map with the varying of input voltage, we select below value of: $V_{in} = 22V,\ 28V, 31.5V, and\ 33V$, to see how the chaos evolute from one to other. the other circuit elements will be R=22Ω, L=20mH, C=47uF, fs =2500Hz.

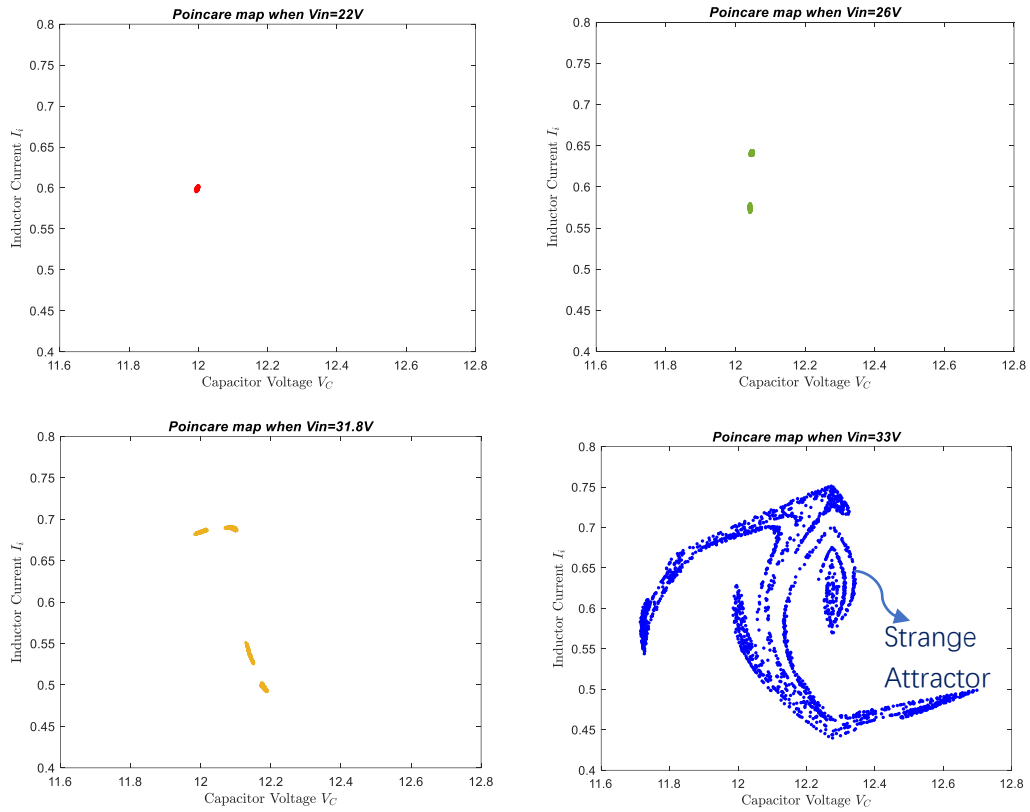

Figure 2.5 Poincaré map for (a)$V_{in} = 22V$ (b) $V_{in} = 26V$ (c) $V_{in} = 31.5V$ (d) $V_{in} = 33V$

It can be clearly observed that when $V_{in} = 22V$ there is only one dot on the phase portrait, as the V_{in} increased to 26V, the strange attractor evolute to two, this phenomenon replicate the analysis of bifurcation diagram of period-doubling bifurcation, as the V_{in} keeps increasing, strange attractors quickly replicate and eventually become chaotic as shown in the figure 2.5(d).

2.4 Theoretical analysis using iterative mapping

Now, we consider establishing a discrete iterative mapping (Poincaré map) and perform stability analysis through the calculation of eigenvalues.

Using the method of stroboscopic mapping, the circuit state variables are discretized, that is, sampling is performed every nT_s time, writing as:

$$x_n = x(nT_s) = [Vo(nT_s), i_L(nT_s)]^T \quad 2.11$$

The operating waveform of the converter is shown in Figure 2.5(a), in one cycle (such as $kT_s \sim (k+1)T_s$) the converter will experience 2 different phases:

(1) When $t = t_n \sim t_{n+\bar{d}}$, switch is in "off state", when this interval ends, the state-variable is $x_{n+\bar{d}}$.

$$x_{n+\bar{d}} = f_{off}(x_n, \bar{d}_n) = N_{off}(\bar{d}_n)x_n + M_{off}(\bar{d}_n)V_{in} \quad 2.12$$

(2) When $t = t_{n+\bar{d}} \sim t_{n+1}$ switch is in "on state", when this interval ends, the state-variable is x_{n+1}.

$$x_{n+1} = f_{on}(x_{n+\bar{d}}, \bar{d}_n) = N_{on}(1-\bar{d}_n)x_{n+\bar{d}} + M_{on}(1-\bar{d}_n)V_{in} \quad 2.13$$

Combining (2.12, 2.13), we can obtain the iterative mapping in the form of:

$$x_{n+1} = f(x_n, \bar{d}_n)$$

$$= N_{on}(1-\bar{d}_n)N_{off}(\bar{d}_n)x_n + [N_{on}(1-\bar{d}_n)M_{off}(\bar{d}_n) + M_{on}(1-\bar{d}_n)]V_{in} \quad 2.14$$

Where,

$\bar{d}_n = 1 - d_n$ (1- duty cycle)

$N_{on}(1-\bar{d}_n) = e^{A_{on}dT_s}$

$M_{on}(1-\bar{d}_n) = A_{on}^{-1}(e^{A_{on}dT_s} - I)B_{on}$

$N_{off}(\bar{d}_n) = e^{A_{off}\bar{d}T_s}$

$M_{off}(\bar{d}_n) = A_{off}^{-1}(e^{A_{off}\bar{d}T_s} - I)B_{off}$

In addition, we need to derive the duty cycle function, which requires finding the relationship between the switching instant and the state variable. To fully understand the exact switching timing, the $S(\bar{d}_n)$ should be expand and correspond with state-variables, this tie relies on:

$$S(\bar{d}_n) = [K\ 0]\begin{bmatrix} V_o(\bar{d}_n T_s) - V_{ref}(\bar{d}_n T_s) \\ i_L(\bar{d}_n T_s) \end{bmatrix} - V_L - (V_U - V_L)\bar{d}_n T_s$$

$$= [K\ 0]\left[N_{off}(\bar{d}_n)x_n + M_{off}(\bar{d}_n)V_{in}\right] - KV_{ref} - V_L - (V_U - V_L)\bar{d}_n T_s \quad 2.15$$

Therefore, function $S(\bar{d}_n) = 0$ defines the timing of switching, where $S(\bar{d}_n) < 0$ the mosfet is on, otherwise mosfet is off.

$$\frac{\partial s}{\partial \bar{d}_n} = [K\ 0]\left[A_{on}T_s N_{on}(1-\bar{d}_n)x_n + T_s N_{off}(\bar{d}_n)B_{off}V_{in}\right] - (V_U - V_L)T_s \quad 2.16$$

$$\frac{\partial s}{\partial x_n} = \lfloor K\ 0 \rfloor N_{off}\left(\bar{d}_n\right) \tag{2.17}$$

Also, we can calculate the $\frac{\partial s}{\partial \bar{d}_n}$ and $\frac{\partial s}{\partial x_n}$, as shown in (2.16, 2.17), which is significant for further calculation, because the Jacobian matrix is an implicit function of $S(\bar{d}_n)$.

The iteration map could help to study the stability of the system, we can calculate the eigenvalues near the equilibrium point, analyze the instability process of the regular state of the system when some parameters change.

Let the jacobian matrix as $Jacobian(x_n, \bar{d}_n)$, then it will be:

$$Jacobian(x_n, \bar{d}_n) = \frac{\partial x_{n+1}}{\partial x_n} = \frac{\partial f}{\partial x_n} - \frac{\partial f}{\partial \bar{d}_n}\left(\frac{\partial s}{\partial \bar{d}_n}\right)^{-1}\frac{\partial s}{\partial x_n} \tag{2.18}$$

Where,

$$\frac{\partial f}{\partial x_n} = N_{on}\left(1-\bar{d}_n\right)N_{off}\left(\bar{d}_n\right) \tag{2.19}$$

$$\frac{\partial f}{\partial \bar{d}_n} = \left[\frac{\partial N_{on}\left(1-\bar{d}_n\right)}{\partial \bar{d}_n}N_{off}\left(\bar{d}_n\right) + N_{on}\left(1-\bar{d}_n\right)\frac{\partial N_{off}\left(\bar{d}_n\right)}{\partial \bar{d}_n}\right]x_n$$

$$+\left[\frac{\partial N_{on}\left(1-\bar{d}_n\right)}{\partial \bar{d}_n}N_{off}\left(\bar{d}_n\right) + N_{on}\left(1-\bar{d}_n\right)\frac{\partial M_{off}\left(\bar{d}_n\right)}{\partial \bar{d}_n} + \frac{\partial M_{off}\left(\bar{d}_n\right)}{\partial \bar{d}_n}\right]V_{in} \tag{2.20}$$

Then the eigenvalue for the equilibrium point can be calculated as:

$$det\left[\lambda \mathrm{I} - Jacobian(x_n, \bar{d}_n)\right]\Big|_{x_n = x_Q, \bar{d}_n = \bar{d}_Q} = 0 \tag{2.21}$$

Where the x_Q, $\bar{d}_Q$ are the equilibrium point of the iterative mapping, it could be obtained by simulate the iterative mapping in nT_s series until the system goes stable.

Jacobian matrix stability criteria

Characteristic multipliers are the eigenvalues of the Jacobian of a discrete-time iterative system, the system is locally stable if all the characteristic multipliers have a magnitude of less than 1 (in unity cycle); when the first multiplier go out of the unity

cycle, the bifurcation begins, the eigenvalue of the discrete-time map $f[f(x_n, A)]$ is set at the -1.

Using V_{in} as the bifurcation parameter, we can plot the eigenvalues of the Jacobian matrix for the specific iterative map, as shown in figure 2.6.

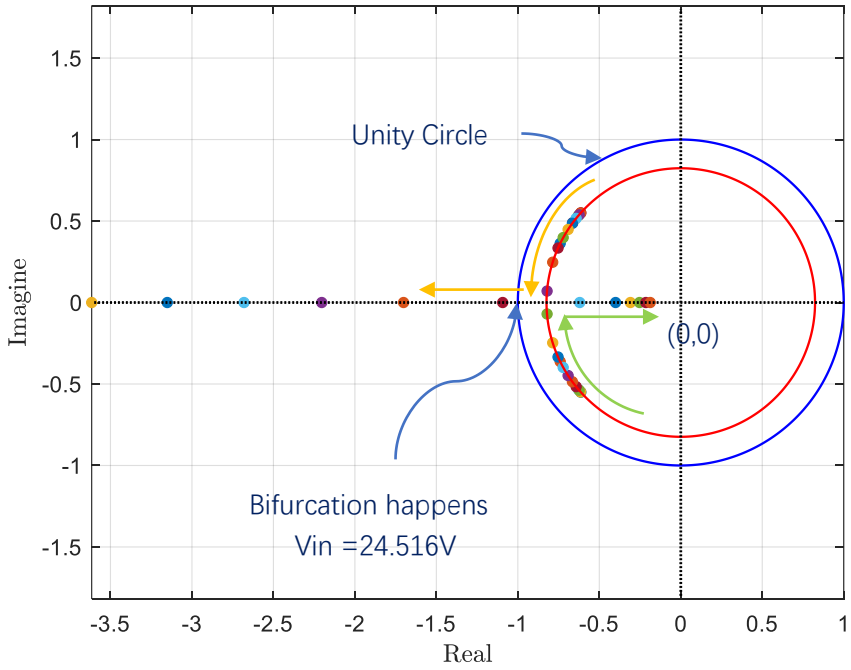

Figure 2.6. loci of characteristic multipliers as V_{in} varies

As shown in Figure 2.6, as the input voltage V_{in} increases, the two eigenvalues, one at second quadrant and one at third quadrant, will approach the real axis along a circle with a radius of approximately 0.82. After reaching the real axis, they will be separated. The eigenvalue on the left will finally leave the unit circle, and the corresponding input voltage V_{in} is 24.5 V (verifies the complete state equation using Matlab), which indicates that the 1-cycle of the converter begins to destabilize, and a first fork bifurcation occurs.

2.5 Complex behavior verification using PSIM

Finally, we can use circuit analysis tools like PSIM to perform the above analysis, the result data was stored in .cvs format files and plot in the matlab, using state space

phase portrait to perform the verification result, as shown in figure 2.7 below. Apart from different V_{in}, all the circuit elements are identical

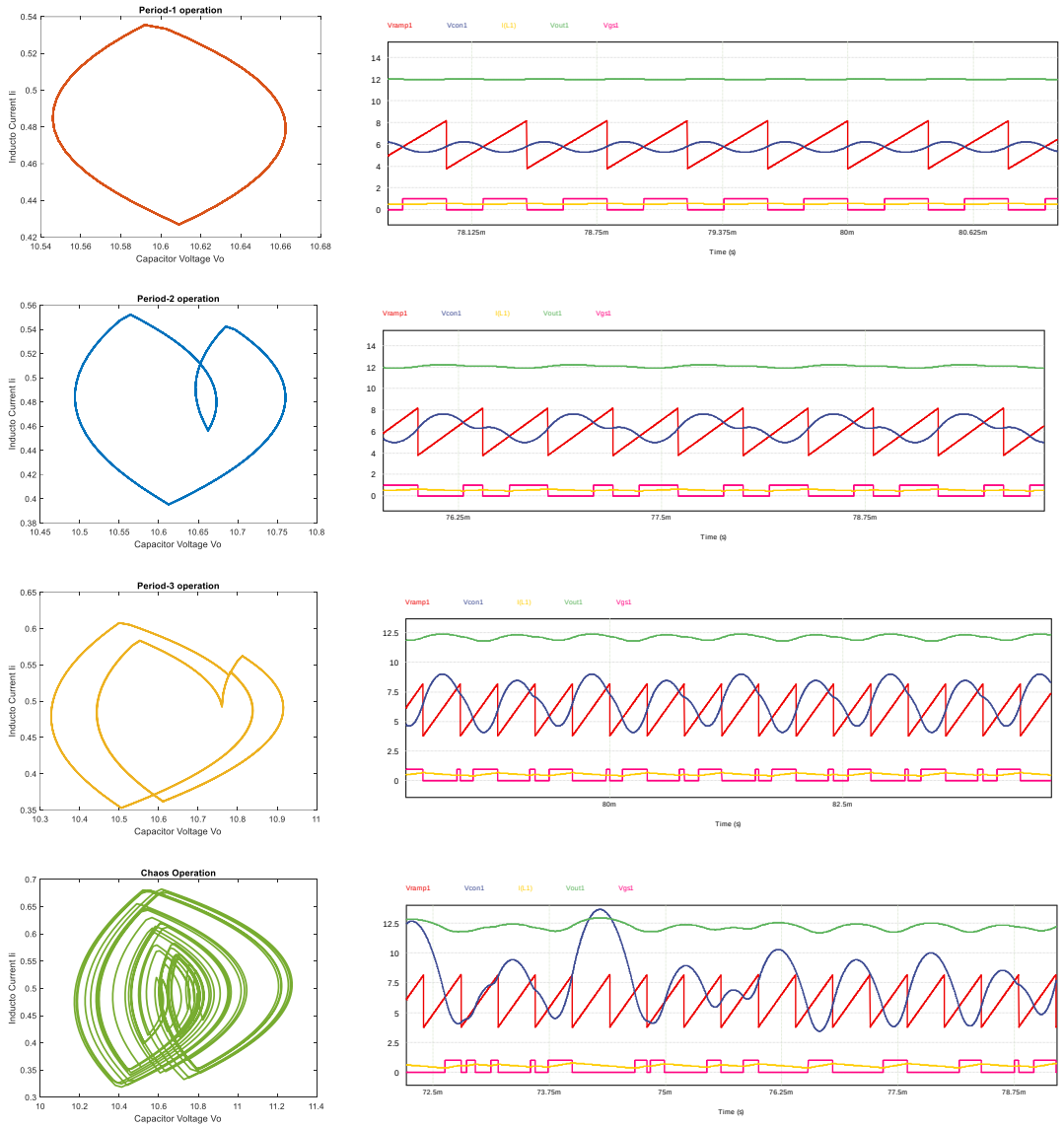

Figure 2.7. Phase portrait and key waveform as V_{in} varies – under PSIM simulation (a) $V_{in} = 20V$ (b) $V_{in} = 25V$ (c) $V_{in} = 30V$ (d) $V_{in} = 35V$

We also chose a particular condition of V_{in}=27V, R =22Ω, L=20mH, C=47uF, fs=2500Hz, K=8.2, to compare the result of matlab with PSIM, the result shows satisfying consistence in figure 2.8, this further verify the accuracy of complete state equation model.

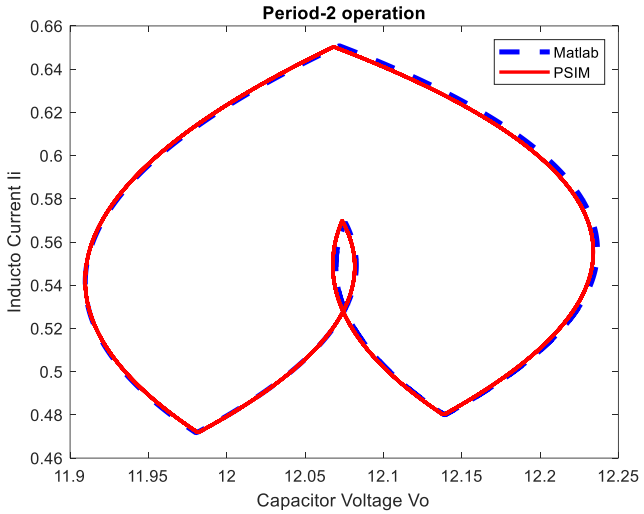

Figure 2.8. Comparation for PSIM and Matalab under a same working condition

3. Complex behavior and its analysis in DCM VCM buck converter

In the previews section, analyzing for CCM buck converters with both complete state equation and discrete iterative map have been detailed described. or the case of discontinuous conduction mode buck converters, the situation will be very similar.

Since complete sate equation methods has been verified its accuracy, we leave this method open for the following analysis, only concentrate on the how to generate the iterative mapping.

Before analysis there are some constrains should be noted first, firstly, as shown in (3.1), the inductance L of the DCM buck converter must be small enough to keep the circuit works in discontinuous-mode; secondly since the solution to each of state can be expressed explicitly in terms of the respective transition matrix, simulation of exact time-domain wave forms is possible using the below piecewise switched model. The following simulations will be based on this model.

$$L < \frac{(1-D)RT_s}{2} \tag{3.1}$$

Where the D, R, T_s, are the Duty cycle, switching frequency, and load resister value of the buck converter, respectively.

3.1 Discrete iteration mapping for DCM Buck

The procedure for deriving iterative maps is conducted as follows. We still need to derive the state equations for the system in advance, assuming the state-variables as $x = [Vo \;\; i_L]^T$, write down the state equations for all involving circuit topologies:

$$\dot{x} = \begin{bmatrix} -/RC & 1/C \\ -1/L & 0 \end{bmatrix} x + \begin{bmatrix} 0 \\ 1/L \end{bmatrix} V_{in} = A_1 x + B_1 V_{in} \quad (t_n < t < t_n + t_1) \tag{3.2}$$

$$\dot{x} = \begin{bmatrix} -/RC & 1/C \\ -1/L & 0 \end{bmatrix} x + \begin{bmatrix} 0 \\ 0 \end{bmatrix} V_{in} = A_2 x + B_2 V_{in} \quad (t_n + t_1 < t < t_n + t_1 + t_2) \tag{3.3}$$

$$\dot{x} = \begin{bmatrix} -/RC & 0 \\ 0 & 0 \end{bmatrix} x + \begin{bmatrix} 0 \\ 1/L \end{bmatrix} V_{in} = A_3 x + B_3 V_{in} \quad (t_n + t_1 + t_2 < t < t_{n+1}) \tag{3.4}$$

Where the matrix A_i and B_i are the coefficient matrix of the system, t_1, t_2, t_3, are the three different operation intervals for DCM buck converter, they are defined as follows:

$$t_1 = d_{1n}T_s\ (when\ inductor\ current\ is\ near - linearly\ increase)$$

$$t_2 = d_{2n}T_s\ (when\ inductor\ current\ is\ near - linearly\ derease)$$

$$t_3 = d_{3n}T_s\ (when\ inductor\ current\ is\ exhausted\ and\ equals\ 0\ )$$

Obviously, we have $d_{1n} + d_{2n} + d_{3n} = 0$ for any cases, then we can solving the first order differential equation in (3.2, 3.3, 3.4), to generate the time domain expressions for the state-value when each state ends, after simplification and substitution as performed in section 2.4, we can obtained the following iterative map:

$$x_{n+1} = f(x_n, d_{1n}) = N_3\,(d_{3n})N_2\,(d_{2n})N_1\,(d_{1n})x_n$$
$$+[N_3\,(d_{3n})N_2\,(d_{2n})M_1(d_{1n}) + N_3\,(d_{3n})M_2(d_{2n}) + M_3(d_{3n})]V_{in} \qquad 3.5$$

Where each coefficient matrix will be (i = 1,2,3):

$N_i\,(d_{in}) = e^{A_i d_{in} T_s}$

$M_i\,(d_{in}) = A_i^{-1}\,(e^{A_i d_{in} T_s} - I)B_i$

It should note that the d_{in} (i=1,2,3) is a time varying parameter corresponding to the sate-variables x, as the control unit shows in the figure 3.1, in VCM buck converter, we have:

$$d_{1n} = D - K\left(Vo_n - V_{ref}\right) \qquad 3.6$$

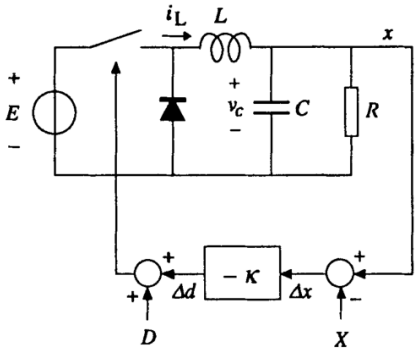

Figure 3.1 Circuit diagram of the DCM buck converter

Approximation in discrete iteration mapping

Clearly this is not an easy mapping we could calculate, so we can use some enforcing conditions that applying for DCM buck specifically [6], since the switching period is much longer than the capacitance-load-resistance time constant in DCM buck converters, for the inductor value at each switching iteration begins, we have $i_n = i_L(t_n) = 0$, accordingly, the duty cycle has the relation of:

$$\frac{d_{2n}}{d_{1n}} = \frac{V_{in} - Vo}{Vo} \tag{3.6}$$

Besides, rather than solving the transition matrix $N_i(d_{in})$, $M_i(d_{in})$, a finite series approximation can be adopted to decrease the calculation complexity, in fact the first two terms is accurate enough for the evaluation of stability, which can be written as:

$$e^{A_i t} = I + A_i t + \frac{1}{2}(A_i t)^2 + \frac{1}{3}(A_i t)^3 + \cdots \tag{3.7}$$

With these two particulars constrains, and focus on one part of state variables ($i_n = 0$ is a constant could be overlooked, so we only need to observe Vo_n), we can simplify and approximate the system to the following form:

$$Vo_{n+1} = g(Vo_n, d_{1n}) = \alpha Vo_n + \beta \frac{d_{1n}^2 V_{in}(V_{in} - Vo_n)}{Vo_n} \tag{3.8}$$

Where the coefficients are:

$$\alpha = 1 - \frac{T_s}{RC} + \frac{{T_s}^2}{2(RC)^2}, \quad \beta = \frac{R{T_s}^2}{2LCR}$$

Also, it should be reminded that d_{1n} will be substituted by h_{1n} because the duty cycle could saturate, thus we add another constrains as:

$$h_{1n} = \begin{cases} 0 & when\ d_{1n} < 0 \\ d_{1n} & for\ 0 < d_{1n} < 1 \\ 1 & when\ d_{1n} > 1 \end{cases} \tag{3.9}$$

Since the system is open loop stable, so $Vo_{n+1} = Vo_n$ when $d_{1n}^2 \to D$, then we can calculate the duty cycle based on known circuit parameters:

$$D = \sqrt{\frac{(1-\alpha){Vo_n}^2}{\beta V_{in}(V_{in} - Vo_n)}} \tag{3.10}$$

Set the Vo_n as the reference value V_{ref} as we desired, then we will have all the parameters we need to complete the discrete iterative map.

3.2 Stability analysis cobweb map and bifurcation diagram

As soon as the iterative mapping is constructed, we can use the virtualization tools to analysis the stability of the system. We chose cobweb map and bifurcation diagram as our visualizing tools; in fact, these two methods are mutual equivalent in mathematical.

The circuit elements value for the analyze are $V_{in} = 33V$, R =12.5Ω, L=208uH, C=222uF, fs=3000Hz, $V_{ref} = 25V$. the discrete iteration mapping predicts feedback gain value will bifurcate the system.

a). System behavior predicts using cobweb map

Additional reminder for cobweb map is that the selection of initial condition, since it was produced by combining the iterative map in (3.8) and the duty cycle constrain in (3.6), and this constrain is only valid when $0 < d_{1n} < 1$, thus the initial condition should not deviate too much from the equilibrium when system is finally stable. See attached documents, we chose a very close initial condition of $Vo_1 = 24V$, only after 1-2 iteration, the discrete state value will drop into the fixed point or the limit orbits.

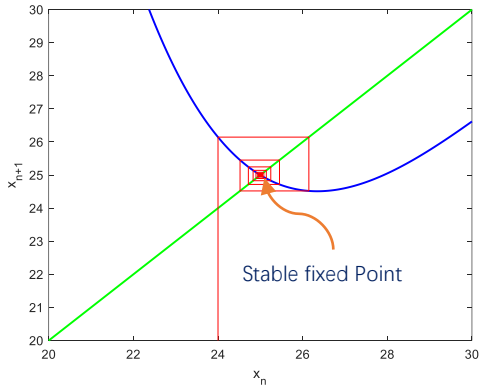

(a) $K = 0.1$

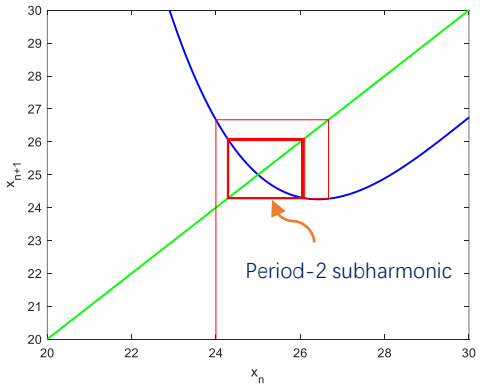

(b) $K = 0.13$

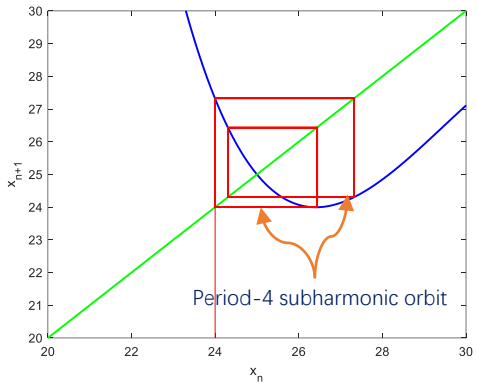

(c) $K = 0.165$

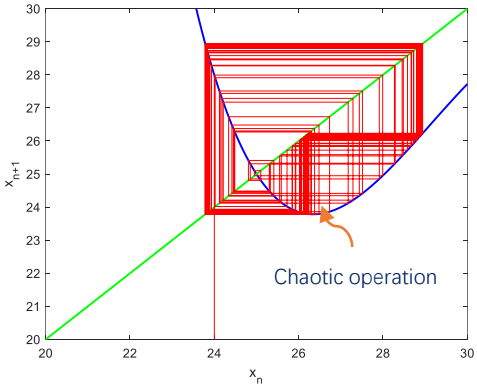

(d) $K = 0.2$

Figure 3.2 Cobweb map for the DCM buck converter when feedback Gain varies
(a) $K = 0.1$ (b) $K = 0.13$ (c) $K = 0.165$ (d) $K = 0.2$

From the cobweb map we can find that with the increasing of feedback gain, the output voltage will go through stable, period-doubling, period-4 and finally goes chaotic, indicating that inappropriate large feedback gain may cause system unstable, but the threshold for behavior evolution is still unknown, so we need bifurcation diagram to further predicts the change.

b). System behavior predicts using bifurcation diagram

By substituting the known circuit parameters to the simplified iterative mapping in (3.8), we can rewrite in numerical term:

$$Vo_{n+1} = g(Vo_n, d_{1n}) = 0.8872Vo_n + 1.202\frac{h_{1n}^2 33(33 - Vo_n)}{Vo_n} \qquad 3.11$$

$$h_{1n} = \begin{cases} 0 & when\ d_{1n} < 0 \\ d_{1n} = 0.4713 - K(Vo_n - 25) & for\ 0 < d_{1n} < 1 \\ 1 & when\ d_{1n} > 1 \end{cases} \qquad 3.12$$

As shown clearly, the system has a stable fixed point in the sub-critical case, and a stable subharmonic orbit in super-critical cases, and first bifurcate at about 0.136; when the feedback gain is grater then 0.17 approximately, the system will go chaotic. From the bifurcation diagram, the bifurcation threshold can be easily estimated.

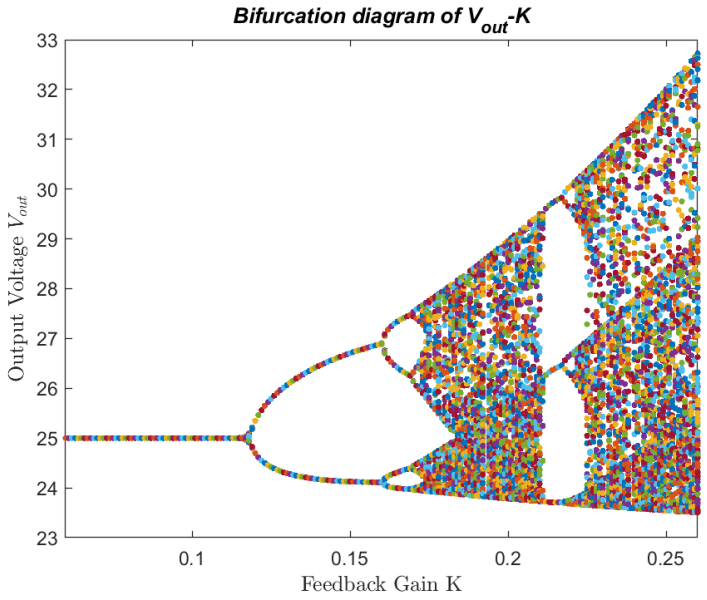

Figure 3.3 Bifurcation diagram using the approximate iterative mapping of parameter K

3.3 Determine threshold for the first fork bifurcation

In terms of the stable closed-loop system with one single steady-state fixed point, the Taylor series around the equilibrium is a helpful tool to determine the threshold of bifurcation happens:

$$\Delta Vo_{n+1} = \sum_{k=1}^{\infty} \frac{1}{k!} \frac{\partial g(Vo_n)}{\partial {Vo_n}^k}\bigg|_{Vo=Vref} (\Delta Vo_n)^k \qquad 3.13$$

Assuming $0 < d_{1n}$<1, then we can rule out the saturation nonlinearity, before the first fork bifurcation happens, the system should strictly stable according to Floquet theory, therefore, after omitting the high-level terms (if don't omitting then the threshold will be slightly larger):

$$\left|\frac{\partial Vo_{n+1}}{\partial Vo_n}\right| = \left|\frac{\partial g(Vo_n)}{\partial Vo_n}\bigg|_{Vo=Vref}\right| \leq 1 \qquad 3.14$$

After simplifying (3.14), we can obtain the approximate characteristic multiplier boundary region, this can be written as:

$$\left|\alpha - \beta \frac{DV_{in}\left[2KV_{ref}\left(V_{in} - V_{ref}\right) + DV_{in}\right]}{{V_{ref}}^2}\right| \leq 1 \qquad 3.15$$

After calculation we can obtain ***K*c=0.1335**, go back to the bifurcation plot using iterative map, the first fork bifurcation can be predicted accurately.

3.4 Complex behavior verification using PSIM

Accordingly, we can use PSIM to perform the above analysis, the result data was stored in .cvs format files and plot in the Matlab, using state space phase portrait to perform the verification result, as shown in figure 3.4 below.

Like CCM buck converter, DCM buck converter can go through bifurcation with multiple parameters, we only choose the feedback gain changing from 0.1~0.2 to verify our analysis in section 3 above, the state variables will go through one/two/four period and finally lead to chaos as predicted, it confirmed the accuracy of the modeling of iterative mapping and once again give a promising result.

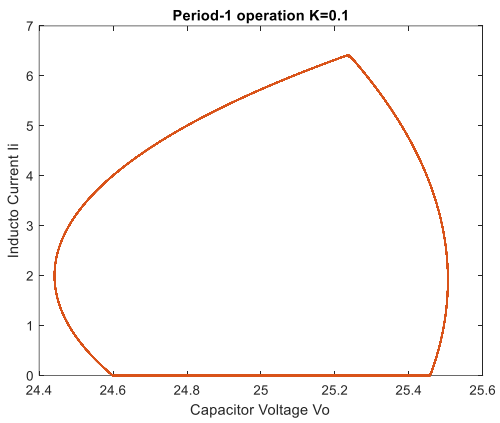

(b) $K = 0.1$

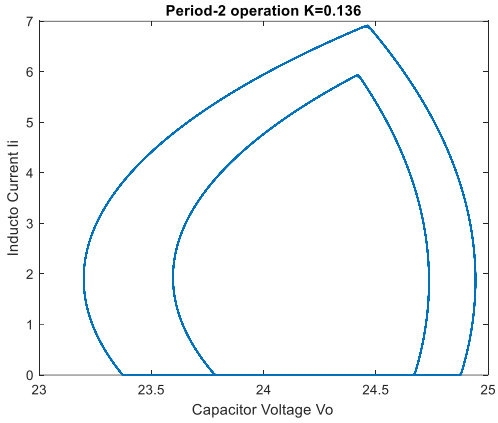

(b) $K = 0.136$

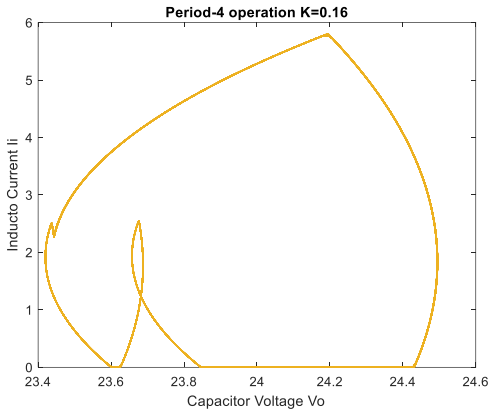

(c) $K = 0.16$

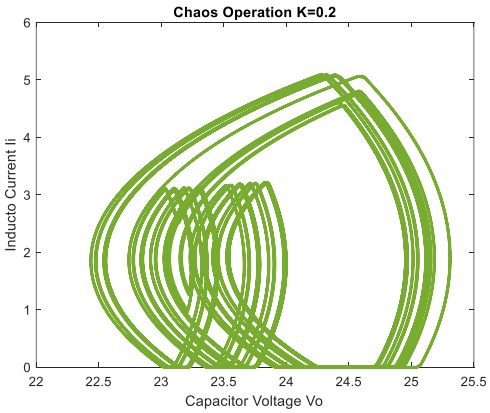

(d) $K = 0.2$

Figure 3.4 Phase portrait and key waveform as V_{in} varies – under PSIM simulation
(a) $K = 0.1$ (b) $K = 0.136$ (c) $K = 0.16$ (d) $K = 0.2$

4. Possible applications of complex behavior buck converter

Cascade converters in renewable energy generation are usually cascaded from two sub-converters. The output voltage of the front end is usually the ripple dc voltage, which serves as the input voltage of the downstream dc–dc converters. The stability of a dc–dc converter with periodic input ripple voltage can perform chaotic behavior.

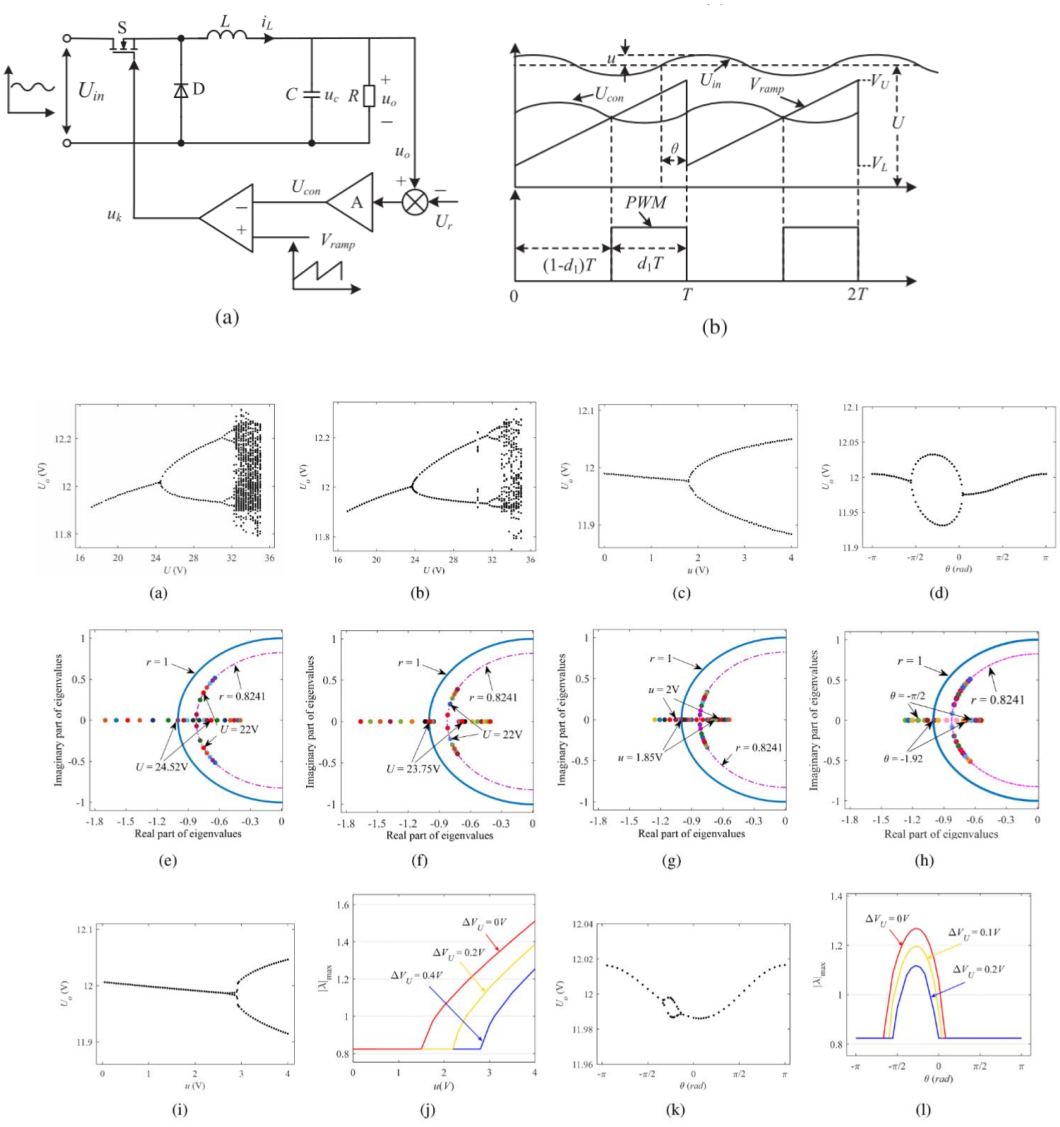

Fig. 2. Evolutionary graphs of bifurcation and eigenvalues. (a) Bifurcation diagram with U_{in} as ripple $u = 0$ V. (b) Bifurcation diagram with U_{in} as ripple $u = 1$ V. (c) Bifurcation diagram with variations of magnitudes of ripples. (d) Bifurcation diagram with different phase shifts θ. (e) Eigenvalues with U_{in} as ripple $u = 0$ V. (f) Eigenvalues with U_{in} when ripple $u = 1$ V. (g) Eigenvalues with variations of magnitudes of ripples. (h) Eigenvalues with different phase shifts θ. (i) Bifurcation diagram with variation of u. (j) Loucs of eigenvalues evolutionary graphs with variation of u. (k) Bifurcation diagram with variation of θ. (l) Loucs of eigenvalues evolutionary graphs with variation of θ.

When the converter is in bifurcation state, the ripple of output voltage and inductance current increases, introducing unpredictable distribution of higher order harmonics even add up stresses to switches or passive components. Therefore, the research in this article can provide better guidance for industrial application of converter.

Thanks to the mathematical tools and various virtualization method, the complex behavior and stability in voltage controlled buck converters can be analyzed by iterative mapping and Jacobian matrix eigenvalues as this report did. The reference paper did the process under the same criteria, by analyzing the bifurcations, Jacobians and characteristic multipliers, the paper draws a good guiding for compensation design and phase shift control.

5. Conclusion

(1) Buck Converter can have very complex behavior coming from varying parameters: Circuit components values, Input voltage; as well as control parameters, feedback gains, and reference.
(2) Two categories of methods are widely used to predicts and analysis the complex behavior: complete numeric state equations and discrete iterative mapping, both has their pros and cons, but mutually complementary in the whole analysis.
(3) Virtualization techniques to observe the chaotic system are various, including loci of multipliers, cobweb map, bifurcation diagram, Poincare map, and phase portrait, these techniques are detailed studied in the report with examples.

6. References

[1] G. C. Verghese, M. E. Elbuluk, and J. G. Kassakian, “A General Approach to Sampled-Data Modeling for Power Electronic Circuits,” IEEE Transactions on Power Electronics, vol. PE-1, no. 2, pp. 76–89, Apr. 1986, doi: 10.1109/TPEL.1986.4766286.

[2] S. Banerjee and K. Chakrabarty, “Nonlinear modeling and bifurcations in the boost converter,” IEEE Transactions on Power Electronics, vol. 13, no. 2, pp. 252–260, Mar. 1998, doi: 10.1109/63.662832.

[3] M. di Bernardo, F. Garefalo, L. Glielmo, and F. Vasca, “Switchings, bifurcations, and chaos in DC/DC converters,” IEEE Transactions on Circuits and Systems I: Fundamental Theory and Applications, vol. 45, no. 2, pp. 133–141, 1998, doi: 10.1109/81.661675.

[4] H. Wu, “Stability Analysis and Control of DC-DC Converters using Nonlinear Methodologies,” p. 187.

[5] S. Pavljasevic and D. Maksimovic, “Using a discrete-time model for large-signal analysis of a current-programmed boost converter,” in PESC ’91 Record 22nd Annual IEEE Power Electronics Specialists Conference, Jun. 1991, pp. 715–721. doi: 10.1109/PESC.1991.162755.

[6] C. K. Tse, “Chaos from a buck switching regulator operating in discontinuous mode,” Int. J. Circ. Theor. Appl., vol. 22, no. 4, pp. 263–278, Jul. 1994, doi: 10.1002/cta.4490220403.

[7] G. Yuan, S. Banerjee, E. Ott, and J. A. Yorke, “Border-collision bifurcations in the buck converter,” IEEE Transactions on Circuits and Systems I: Fundamental Theory and Applications, vol. 45, no. 7, pp. 707–716, Jul. 1998, doi: 10.1109/81.703837.

[8] M. di Bernardo and F. Vasca, “Discrete-time maps for the analysis of bifurcations and chaos in DC/DC converters,” IEEE Transactions on Circuits and Systems I: Fundamental Theory and Applications, vol. 47, no. 2, pp. 130–143, Feb. 2000, doi: 10.1109/81.828567.

[9] Y. Zhou, C. K. Tse, S.-S. Qiu, and F. C. M. Lau, “APPLYING RESONANT PARAMETRIC PERTURBATION TO CONTROL CHAOS IN THE BUCK DC/DC CONVERTER WITH PHASE SHIFT AND FREQUENCY MISMATCH CONSIDERATIONS,” Int. J. Bifurcation Chaos, vol. 13, no. 11, pp. 3459–3471,

Nov. 2003, doi: 10.1142/S0218127403008685.

[10] X. Feng, C. Bi, Y. Xiang, and Q. Zhang, “Dynamical analysis of the DCM buck converter,” in 2013 International Conference on Communications, Circuits and Systems (ICCCAS), Nov. 2013, vol. 2, pp. 442–445. doi: 10.1109/ICCCAS.2013.6765378.

[11] E. Rodríguez Vilamitjana, A. El Aroudi, and E. Alarcón, Chaos in Switching Converters for Power Management. New York, NY: Springer New York, 2013. doi: 10.1007/978-1-4614-2128-3.

[12] H. Wu, V. Pickert, D. Giaouris, and B. Ji, “Nonlinear Analysis and Control of Interleaved Boost Converter Using Real-Time Cycle to Cycle Variable Slope Compensation,” IEEE Trans. Power Electron., vol. 32, no. 9, pp. 7256–7270, Sep. 2017, doi: 10.1109/TPEL.2016.2626119.

[13] W. Hu, R. Yang, X. Wang, and F. Zhang, “Stability Analysis of Voltage Controlled Buck Converter Feed From a Periodic Input,” IEEE Transactions on Industrial Electronics, vol. 68, no. 4, pp. 3079–3089, Apr. 2021, doi: 10.1109/TIE.2020.2982116.

[14] E. Fossas, “Department of Applied Mathematics and Telematics April 30th, 1997.,” p. 264.

[15] H. Wu, “Stability Analysis and Control of DC-DC Converters using Nonlinear Methodologies,” p. 187.

[16] C. K. M. Tse, “Analysis and Control of Power Converters,” p. 43, 2011.